Parametric optimization of sandwich composite footbridge with U-shaped cross-section

Tomasz Ferenc

Gdansk University of Technology, Faculty of Civil and Environmental Engineering

Tomasz Mikulski

Gdansk University of Technology, Faculty of Ocean Engineering and Ship Technology

ABSTRACT

Parametric optimization of sandwich composite footbridge was presented in the paper. Composite footbridge has 14,5 meters long and has U-shaped cross-section with inner dimensions 2,6 x 1,3 meters. The aim of analysis was to minimize the mass of the new footbridge that can lead to minimize the cost of structure. After optimization was conducted, the new structure was compare with the realized one. The results show that while mass can be decreased the state variables of structure like maximum displacement, strain or natural frequency do not change significantly. Moreover, results show that, although the mass is decreased, stiffness of the new structure is even higher.

Optimization and sensitivity analysis, the divisions of theory of designing, provide the designer a significant support. Despite presented optimization, also sensitivity analysis can additionally be effectively used in issues related to strengthening or modernizing structures as well as in the process of identifying quantities describing the computational model.

Keywords: Optimization, sandwich structure, polymer composites, GFRP laminates

1. Introduction

To meet the requirements of today's civil structures, next to traditional materials like steel or concrete new materials are invented and become more commonly used. In order to construct structures which are greater and more durable with lower cost, material itself must have higher strength with decreased mass. To meet these challenges, Fiber Reinforced Polymers (FRP) have emerged to be used in civil engineering structures [1]÷[5]. Considering bridge structures the process of application of composite elements started in 1980s by strengthening and retrofitting of existing structures [6]. Then application of single or more elements in structures occur, like composite decks produced in wet layup process [7] or profiles manufactured in pultrusion [8] to be applied in truss or suspension structures [9]÷[10]. Finally, the last years have allowed the development of new technology, mainly taken from marine or aviation industries. New methods of manufacturing, i.e. infusion, gave great possibilities in forming geometry of single elements or whole structure produced as a single element [11]÷[14]. As the structures made from composites became increasingly popular and due to their novelty, the unprecedented problems with their design occur. Hence the optimization, which was conducted in the paper, started to be widely used tool that is very helpful for structural designer.

Optimization, or design optimization, is a process based on assumed algorithms that generate improved structural design [15]÷[18]. Two types of the problem can be distinguished: topology structure shape optimization and parametric optimization.

The first group, the topology structure shape optimization, focuses on searching the new geometry of the system. The design variables describe the new shape of structure. Paper [19] consider designing the shape and thickness of shell structures consisting of orthotropic materials for various boundary conditions, while [20] focuses on designing the shape of multiphase composite structure under certain range of excitation frequencies. In paper [21] methodology of

optimization of a cross-section shape of an anisotropic composite structure using a genetic algorithm GA is presented which allowed to increase a specific structural stiffness by 330% comparing to quasi-isotropic stack sequence. Moreover, paper [22] ponders on transverse shear effects in thin walled laminated composite and exhibits the influence of the various numerical shell models and fibre orientations on the optimal shape design. On the other hand paper [23] studies a topology optimization of composite structure taking into account uncertainty with imprecise probability, while paper [24] presents the optimization methods for the design of the multi-scale free-layer damping structure where the objective is the optimal layout due to maximize the structural damping performance. In the process of searching for the optimal solution, sensitivity analysis was used at both micro and macro levels of the system. This is also valuable information for the designer who can follow the individual steps of the optimization procedure.

The second group, parametric optimization, in which the geometry system does not change, consider the parameters describing the structure as design variables. For composite structures, the parametric optimization can lead to obtain the new parameters describing structure without changing its shape generally, i.e. stack sequence of laminates – number and orientation of plies or total thickness of faces or core in sandwich structures. Paper [25] investigate the optimized distribution and stack sequence of composite panels with sub-stiffening under compression to improve the critical buckling load, while paper [26] considers the stability analysis of an axially compressed multi-layered shell panel influenced by a centrally located square cut-out. In structural stability problems, the optimal solution is obtained with respect to active constraints of local and global stability. In this case, it is necessary to examine the possible interaction of these two forms of loss of stability. Such a phenomenon can significantly reduce the value of critical load in relation to the optimal solution. In paper [27] hybrid composite plates and shells were studied to obtained its optimal fiber volume, fiber orientation and stack sequence via multi-scale optimization

framework by means of Discrete Material Optimization DMO taking into account natural frequency. Paper [28] contains the examples of searching the optimal fibers orientation in hyperelastic composite material considering large displacement and rotation. Furthermore, paper [29] proposes a multi-scale optimization strategy for the design of composite fuselage barrel in which the structure was represented by integrating global-local finite element modelling approach. On the other hand, composite sandwich structures become more popular due to its lightweight character and high flexural stiffness. Paper [30] presents the design and optimization of sandwich structure under normal and oblique dynamic load, in which the depth and the cell size of honeycomb core were taken into account as design variables and the objective was to obtain the highest energy absorption capacity. Moreover, in paper [31] parameter optimization of the turbine cascade with honeycomb tip under wind load in a low-speed tunnel was performed. Moreover, paper [32] studies the optimization of sandwich panels with protective cover based on computational mechanics, in which the objective was minimization of deformation caused by blast loading. Additionally, paper [33] investigate the performance of the response of composite repair of steel pipeline subjected to puncture from excavator bucket tooth, taking into account contact, delamination, decohesion or loss of integrity of both composite and steel.

Although, there are many aspects related with composite structures that has to be concerned, statics remain the foundation for civil structure designers. According to European standards, while designing process two states have to be taken into account: Ultimate Limit State ULS and Serviceability Limit State SLS, where considered state variables are assumed as stress and displacement, respectively. Moreover, from the designer point of view, the most desired effect from conducted optimization process can be structure's mass, or weight, minimization which is unequivocal to cost reduction.

In years 2013-2015 the project called FOBRIDGE was realized by Gdansk University of Technology, Military University of Technology in Warsaw and Roma Limited Company [34]. The main aim was to produce whole structure made from composite materials as a single element in one technological process. After the design process that lasted nearly three years and during which many experiments were conducted on various small sized samples like single laminates or sandwich beams [35]÷[36] and after sophisticated experiments with computational model validation conducted on full-sized segment [37]÷[38], the concept was chosen for realization. The structure was entirely manufactured in a single infusion process, which includes dry laying of all structural components, followed by supersaturation of resin under the sack. After that, it was installed and examined in Gdansk University of Technology campus in 2016 including static (short and long-term) [39] and dynamic tests [40]. The tests were aimed to investigate footbridge behavior itself together with computational model validation. Thus, several schemes were performed. Static vertical load, according to European standard EN 1991-2, was applied by means of concrete slabs with weight up to 20565 kg (Fig. 1a) which is corresponds to the load about 5 kN/m^2. Among others, crowd loading was generated as well (Fig. 1b).
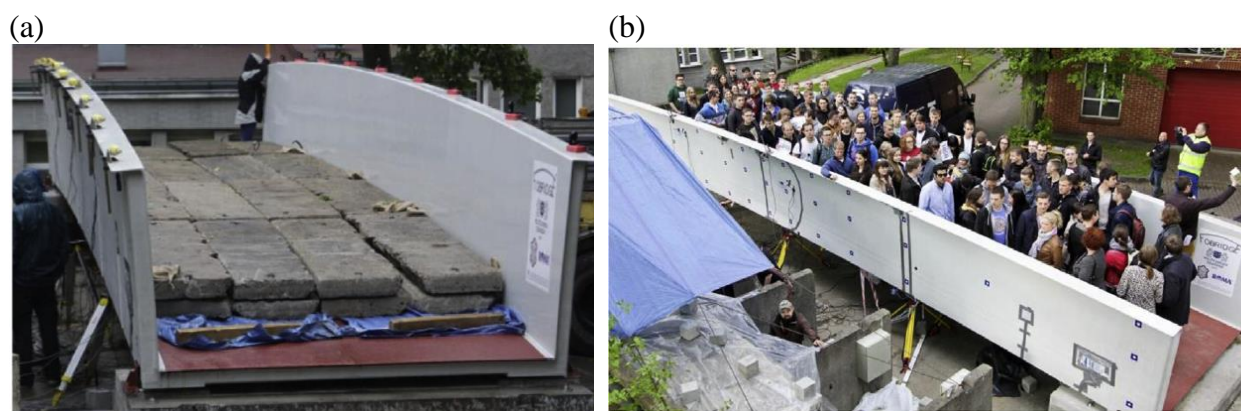
(a)   (b)

Fig. 1. Composite footbridge during tests performed in Gdansk University of Technology campus [39]

2. Description of footbridge

Considered footbridge is a sandwich and shell like structure consisting of Glass Fiber Reinforced Polymer (GFRP) multilayered laminate as faces and PET foam as a core. Dimensions of U-shaped cross-section, which were established due to restrictions in Polish and European standards for footbridges for pedestrian and cyclic traffic, are constant along whole length of structure (Fig. 2). Thus the usable width is 2.5 m, total inner width is about 2.6 m, and the height of walls, which are the handrails at the same time, is 1.3 m. Total length of the structure is 14.5 m, while theoretical span length is 14 m.
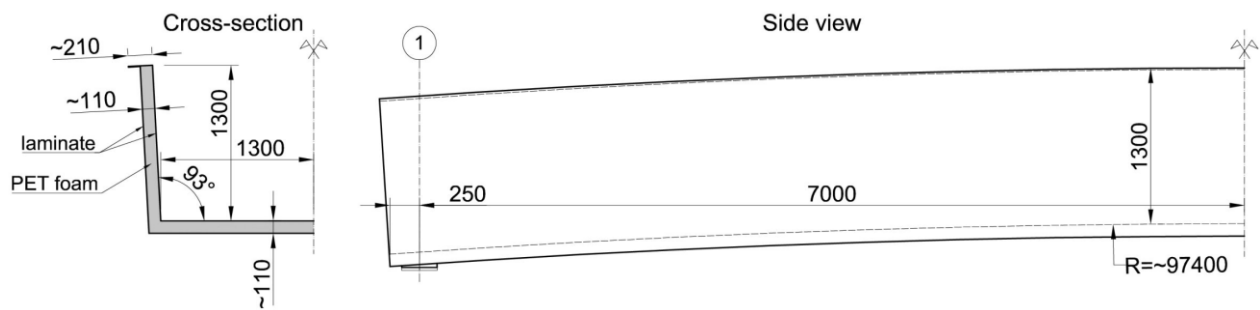

Fig. 2. Dimensions of composite footbridge

The thicknesses of sandwich components are constant all over the structure, hence the core is 10 cm and the faces are 3.978 mm thick, respectively. The faces consist of multilayered laminate which are made of polymer, vinyl ester resin reinforced with stitched glass fabrics. Two types of fabrics were used with fiber orientation [0/90] and [+45/-45] denoted as BAT and GBX respectively, both with the same density 800 g/m^2. The faces are built with six plies, with the following stack sequence [BAT/GBX/BAT$_2$/GBX/BAT] which is synonymous with [(0/90)/(+45/-45)/(0/90)]$_S$ thus laminate are symmetric.

The stack sequence of structure were assumed due to control stress level in a single orthogonal ply of laminate by means of Failure Index (FI) according to Tsai-Wu hypothesis [41]-[42]. For the design purpose, the value of FI was established as about 0.2 in order to avoid any damage in ply

like microcracks [43]-[44]. Above the assumed value of FI the material parameters change their values, i.e. stiffness modulus decrease [37]. The stack sequence given above fulfil this requirement for the load acting on the footbridge according European standard 1991-2.

Material parameters for single ply with the thickness of 0.663 mm are listed in Table 1, and for PET foam in Table 2. Parameters for laminates were determined by Military University of Technology Laboratory in Warsaw [45], while for PET foam were given by producer.

Table 1. Material parameters of single GFRP ply [45]

Parameter		Description	value	unit
E_1	E_2	longitudinal (1) and transverse (2) elastic moduli	23.4	[GPa]
v_{12}		Poisson's ratio	0.153	[-]
G_{12}		in-plane shear modulus	3.52	[GPa]
G_{13}	G_{23}	transverse shear moduli	1.36	[GPa]

Table 2. Material parameters of PET foam

Parameter	Description	value	unit
E	elastic modulus	70	[MPa]
v_{12}	Poisson's ratio	0.4	[-]

After positive evaluation during tests (Fig. 1), the structure was installed over Radunia River near the city of Gdańsk and are used by pedestrians and cyclists (Fig. 3). Steel elements on outer facings of walls are only decoration and are installed due to requirement of conservator-restorer as a reference to a previous historical footbridge located in the same place.

As the footbridge was investigated with positive results, the aim of this paper in to performed its optimization. Due to technological requirements for infusion process, the assumption was made that only thickness of faces of sandwich structure can be modified corresponding to the initial structure. PET foam used as the core is manufactured in selected thicknesses only. The variation of its thickness would cause abrupt change in thickness of entire sandwich structure. Hence, during manufacturing in infusion process, liquid resin would meet difficulties in supersaturation all dry

laying components. Moreover, the use of core with different thickness may significantly reduce the bearing capacity of sandwich due to discontinuities of faces that occur in places where the thickness of core is changed.
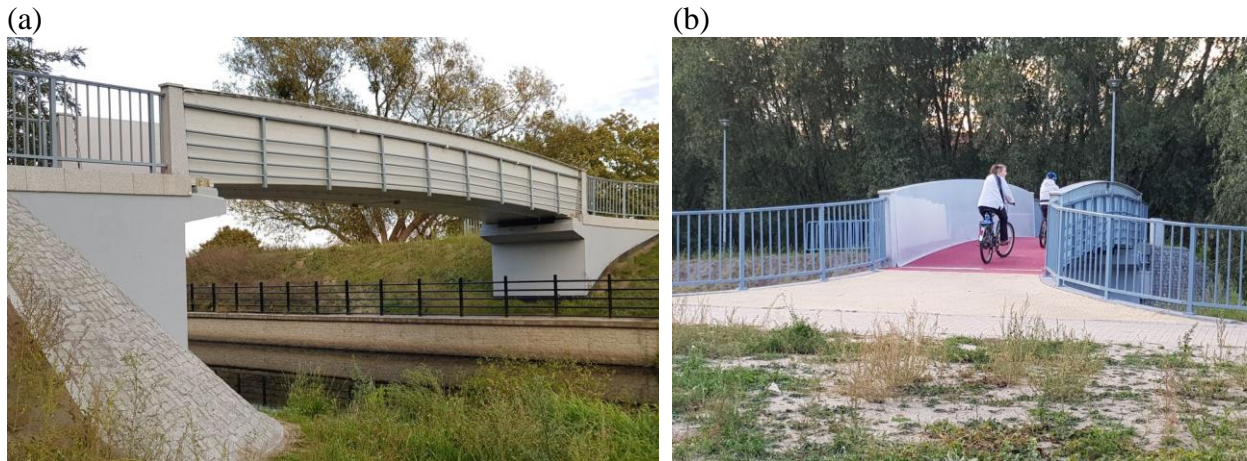
(a)

(b)

Fig. 3. Composite footbridge over Radunia River near the city of Gdańsk (Poland)

3. Numerical models of footbridge and its validation

Numerical models of composite footbridge were created in FEMAP with NX Nastran commercial software by means of Finite Element Method (FEM). The first step was to choose the right model to represent real structure most accurately. Several methods of modeling composites are valid including three dimensional continuum formulations or simplified two dimensional ones where the thickness is reduced, i.e. Layerwise modeling (LW) or Equivalent Single Layer (ESL) [46]-[47]. After experimental validation tests conducted on full-scaled segment with only length reduced to 3 meters [37], hybrid model was chosen to simulate sandwich structures behavior where the core was built by three dimensional solids and faces by two dimensional shells computed by means of ESL theory. Hence, model ORTHO6 was created that represent six-layered laminates as it is – as a shell with six plies. Additionally, two models ISO and ORTHO was studied as well, in

which six-layered laminate was simplified to a single ply shell with isotropic and orthotropic characteristic respectively.

Because of symmetry, only quarter of structure was analyzed (Fig. 4). Loading was assumed according to European Standard EN 1991-2. Hence surface loading $q_t = 5$ kN/m^2 was applied on platform deck (Fig. 4a). Due to assumed mesh size, in which characteristic dimension of finite element was about 25 mm, total number of elements was 210.207 while total number of nodes was 178.638. Four-node shell elements were used to describe laminates and eight-node solid elements were used to model foam.

(a) (b)
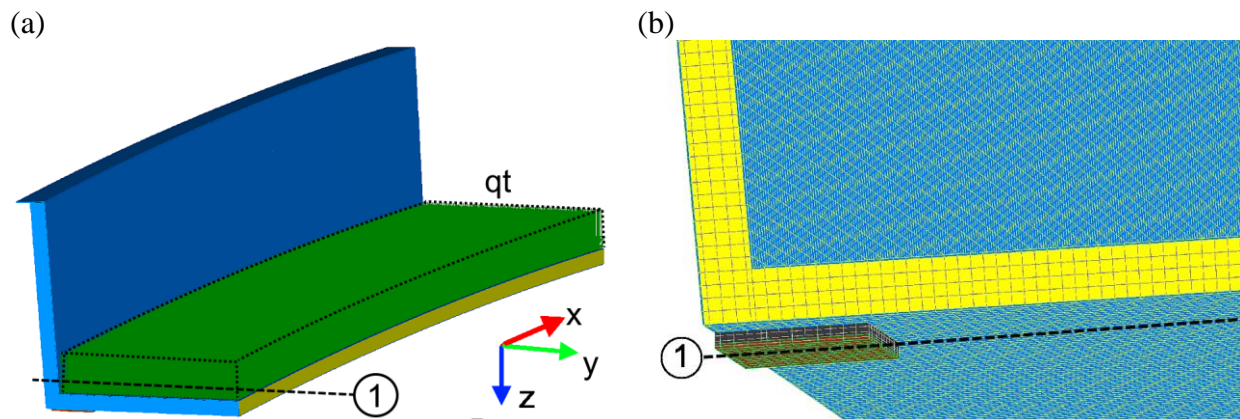
Fig. 4. Model of analyzed footbridge: (a) overall view with loading, (b) detail of bearing with FEM mesh size

All three models were compared to the real structure. Values of measured vertical displacement in the mid-span length v_z, minimum compressive longitudinal strain in handrail ε_{x1} and maximum tensile transverse strain in platform deck ε_{y2}, taken after [39], were compared with the ones obtain from numerical models and listed in Table 3. Additionally, results obtained from model SL, in which entire sandwich was simplified and modeled as a single ply by means of ESL theory, was presented after [39].

Table 3. Comparison of values obtained from experiment and various models

Model	v_z [mm]	ε_{x1} [μm/m]	ε_{y2} [μm/m]
Experiment [39]	31.4	-885	345
SL [39]	41.68	-1302.7	482.3
ISO	34.35	-1048.9	477.9
ORTHO	37.64	-1081.1	497.4
ORTHO6	38.75	-1215.0	507.9

4. Numerical example

4.1. Description of the optimization problem

In this case of the optimization issues, the quantities describing the computational model were divided into two groups:

- parameters - these are quantities that are not subject to change in the process of optimal search for a solution,

- design variables - so-called decision or design variables that may be subject to change within the assumed limits.

The standard problem of parametric optimization can be written as:

$$\min_{\mathbf{x} \in X_d} F(\mathbf{x})$$

$$X_d = \left\{ \mathbf{x} \in R^n : g_i(\mathbf{x}) \leq 0, i = 1, 2, ..., m_1 \; ; g_i(\mathbf{x}) = 0, i = m_1 + 1, m_1 + 2, ..., m \right\} \,, \tag{1}$$

where X_d is feasible region, $\mathbf{x} = \{x_1, x_2, ..., x_n\}^T$ is the design variables vector, n – is the number of design variables, $F(\mathbf{x})$ – is the objective function, $g_i(\mathbf{x})$ – is the i-th constraint function, m – is the number of constraints. Due to inequality constraints that are the most common, the number of constraints of the optimization problem is $m = m_1$.

Two groups of algorithms can be distinguished to solve the problem of parametric optimization:

- zero-order algorithms, often called as gradient-free methods, where only the values of the objective function and constraints are used,

- first-order algorithms, called as gradient-based methods, where in addition to the value of the objective function and constraints also the first derivatives are take into account.

Gradient-free algorithms are divided into two groups: simple search methods and methods of improved directions. Usually in both cases, the problem of searching for a minimum function with constraints is replaced by the problem of searching for minimum of an unconstrained function using the concept of a penalty function. The solution is being searched in steps, while at each step minimum function is achieved in a given direction. The most well-known and widely used procedure is Powell's conjugate direction method for the search of minimum function using the concept of penalty function (Fig. 5).
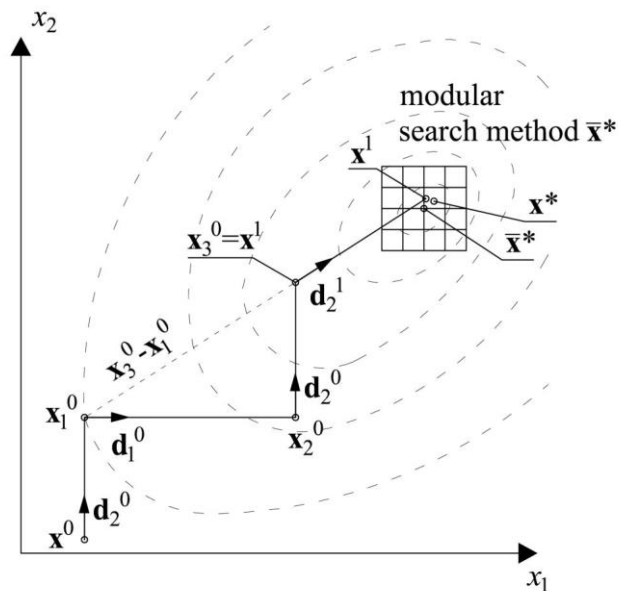
Fig. 5. A concept of Powell's conjugate direction method

The function must be real-valued, of a fixed number of real-valued inputs and does not have to be differentiable. It uses previous stories solutions to create new search directions. N linearly independent search directions are created and performed sequentially in a series of searches along

these directions, starting each time from a previously found point. If the problem is so-called convex problem, the solution is the global minimum.

In gradient-based methods, the gradient at point **x** can be numerically determined using the well-known following formula:

$$\nabla F\left(\mathbf{x}\right) = \begin{Bmatrix} \dfrac{\partial F}{\partial x_1} \\ \dfrac{\partial F}{\partial x_2} \\ ... \\ ... \\ \dfrac{\partial F}{\partial x_n} \end{Bmatrix} \quad , \quad \frac{\partial F\left(\mathbf{x}\right)}{\partial x_i} = \frac{F\left(x_1, x_2, ..., x_i + \Delta x_i, ..., x_n\right) - F\left(x_1, x_2, ..., x_i - \Delta x_i, ..., x_n\right)}{2\Delta x_i} \qquad , \quad (2)$$

On each step the gradient $\nabla F(\mathbf{x})$ can be treated as the first order sensitivity vector of the objective function due to the design variable vector changes $\delta\mathbf{x}$.

The convergence of searching for the minimum point will strongly depend on determining of the starting point - the procedures are well numerically conditioned when the starting point is far from the optimal solution.

Optimal solution of technical problems is usually located on the border of the feasible region. In these case, the Kuhn-Tucker conditions for the minimum point is satisfied

$$-\nabla F\left(\mathbf{x}^*\right) = \sum_{i=1}^{m} \lambda_i \nabla g_i\left(\mathbf{x}^*\right) \qquad , \qquad (3)$$

where $\lambda_i \geq 0$ are Lagrange multipliers (Fig. 6), which are positive only for active constraints.

In optimization issues, the choice of method to solve the problem mainly depends on the functions describing the objective function and the constraints.
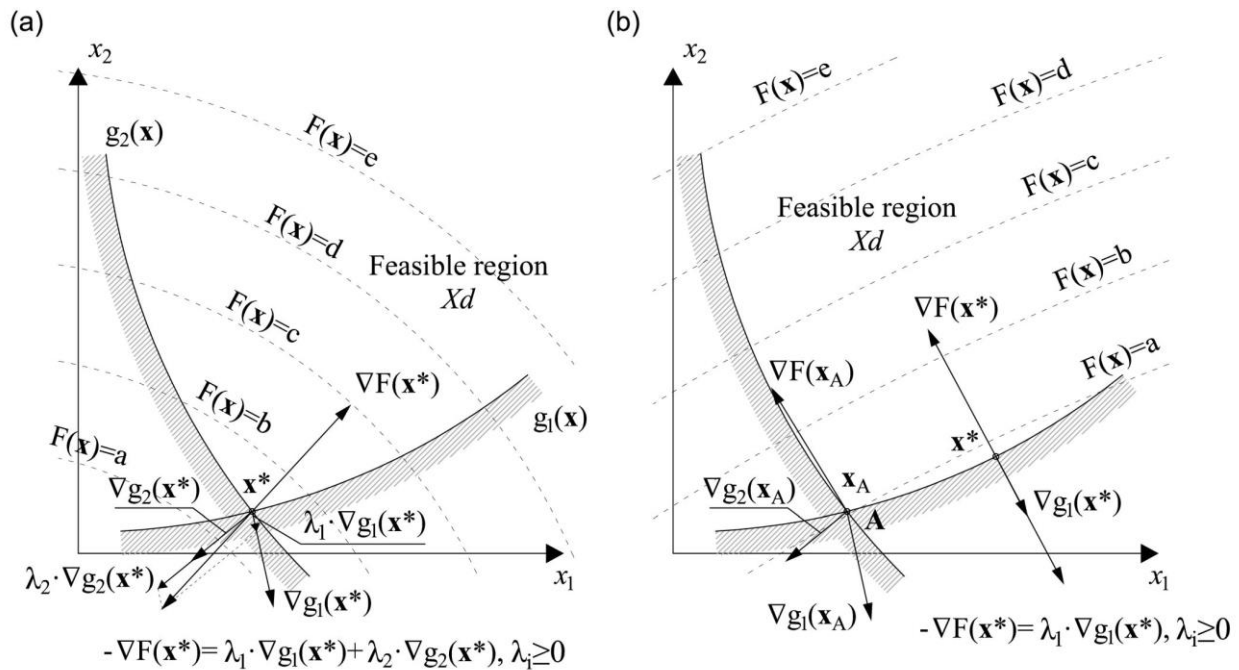
Fig. 6. Kuhn-Tucker conditions for the minimum point

Due to software capabilities and possibility of optimization, in the first step, two models ISO and ORTHO were chosen to provide parametric optimization. In some cases of analysis, multilayered laminates with six or more plies can be simplified to isotropic single ply with mean material parameters. Moreover, model ORTHO were studied as well to provide greater range of comparison.

Both models, ISO and ORTHO, were divided into eight segments: S1÷S8 (Fig. 7). The first one (S1) has 0.5 m long and is located near support. Then, next segments (S2÷S7) have 1 m long, while the last one (S8) which is located near mid-span and has about 0.75 m which results from the total length of structure. Each of eight segments consist of five independent areas, where various types of laminates can be used (Fig. 8): internal and external laminate in the wall (w1 and w2), internal and external laminate in the platform deck (d1 and d2) and laminate in the handrail (h). As

a result, 40 independent areas were obtained. The thickness of laminate in each of 40 areas was assumed as design variables $\mathbf{x} = \left\{ t_1, t_2, \ldots, t_i, \ldots, t_n \right\}^T$.

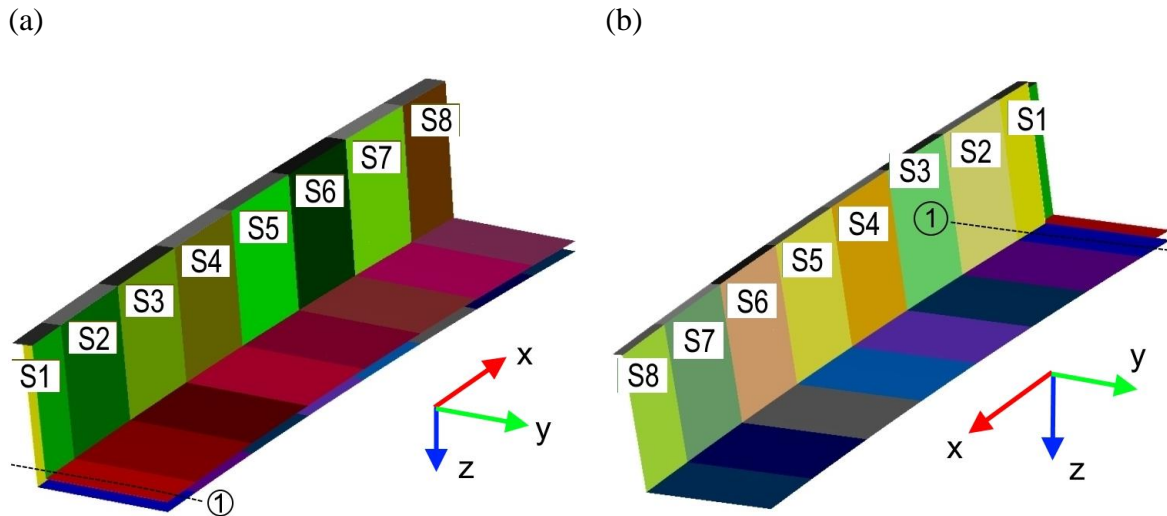(a)   (b)

Fig. 7. Models ISO and ORTHO divided into segments: (a) view from the top on inner laminates, (b) view from the bottom model on outer laminates
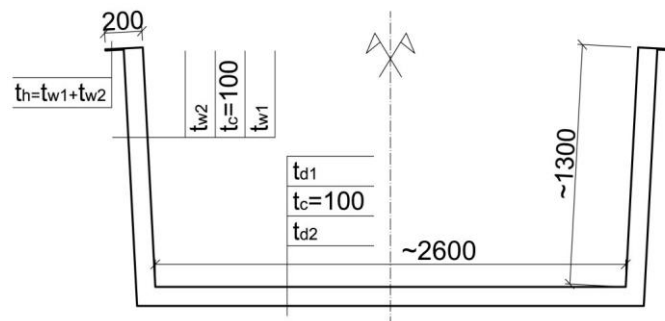

Fig. 8. Cross-section of analyzed footbridge [mm]

In the optimization issues, the quantities describing the computational model were divided into two groups: parameters - these are quantities that are not subject to change in the process of optimal search for a solution and design variables - so-called decision variables that may be subject to change within the assumed limits. In the paper, the laminate thicknesses of the sandwich face in the areas of the separated sections were assumed as design variables. The shape of the footbridge and the parameters of the core are not subject to change. It is therefore a parametric optimization problem.

The standard optimization problem was formulated in accordance with the possible description of the issue available in the FEMAP system. The objective function is the total weight of the laminate:

$$F(\mathbf{x}) = \sum_{i=1}^{n} A_i \cdot t_i \cdot \rho, \tag{4}$$

where $\mathbf{x} = \{t_1, t_2, \ldots, t_i, \ldots, t_n\}^T$ is a vector of design variables, n - number of design variables, A_i - is the field of the i-th section, t_i - is the thickness of the i-th section, ρ - describes the density of the material constant for the whole structure.

The constraints are divided into three groups:

- geometric

$$\begin{aligned} g_i(\mathbf{x}) &= t_{min} - t_i \leq 0 \quad i = 1, \ldots, n \\ g_i(\mathbf{x}) &= t_i - t_{max} \leq 0 \quad i = n+1, \ldots, 2n \end{aligned}, \tag{5}$$

- stress limits

$$\begin{aligned} g_i(\mathbf{x}) &= \sigma_{min} - \sigma_i \leq 0 \quad i = 2n+1, \ldots, 3n \\ g_i(\mathbf{x}) &= \sigma_i - \sigma_{max} \leq 0 \quad i = 3n+1, \ldots, 4n \end{aligned}, \tag{6}$$

- extreme displacement related to footbridge deformation

$$\begin{aligned} g_{4n+1}(\mathbf{x}) &= \delta_{extr} - \delta_d \leq 0 \\ \delta_d &= \frac{l}{300} \end{aligned}. \tag{7}$$

Therefore, the problem of parametric optimization turned out to be significant – with 40 design variables and 161 constraints. The efficiency of achieve the optimal solution that meets all of the constraints set depends on the determining of the starting point. The authors of the work used two variants of starting point selection - initial values of the thickness of the composite faces of

individual sections of the footbridge. The first starting point is from the lower values (t_{min}) while the second from the upper values (t_{max}). Presented results are from the first starting point.

Optimization was conducted in three steps. Nevertheless, the first and the second one can be treated as a tests or theoretical ones, while the third is the right one.

4.2. Results for step I

In the first step, only two constraints were active – geometric and deformation. Limits of design variables t_i were adopted, only for theoretical reasons, in wide range – from $t_{min}=0.1t_0$, which is 10% of initial laminate thickness, to $t_{max}=3t_0$, which is 300% of initial laminate thickness. Although there is no requirements for displacement of bridges made from composite materials, the allowable extreme vertical deflection occurring in the middle of the span was assumed, according to polish standard PN-S-10052-1982 for full-walled beam span of steel road bridge, as $\delta_d=l/300=14.5/300=0.04833$ m, where $l = 14.5$ m is the length of the footbridge. Moreover, that is even more demanding than the allowable deflection according to polish standard PN-S-10042-1991 for concrete footbridges which is $\delta_d=l/200$.

The results of optimization in the form of obtained thickness of i-th laminate areas (i-th design variables) are presented in Fig. 9. As it can be observed, in order to achieve the objective function with assumed constraints, most of the structure areas can have decreased thickness up to the lowest constraints which is 0,3978 mm, which is 10% of the initial value. Only near mid-span length of footbridge, in platform and in handrail, thickness is greater than that lowest limit. As a result of thickness reduction, stress values in laminates significantly increased, what is presented in Fig. 10. The values of longitudinal stress increased up to nearly 5 times comparing to initial model, i.e. from the range of $\langle -25,20\,;13,40 \rangle$ MPa to $\langle -56,37\,;64,54 \rangle$ MPa for model ISO and from

$\langle -26,02\,;16,64\rangle\,$MPa to $\langle -56,06\,;77,06\rangle\,$MPa for model ORTHO. Thus, another limits has to be provided.

(a)   (b)

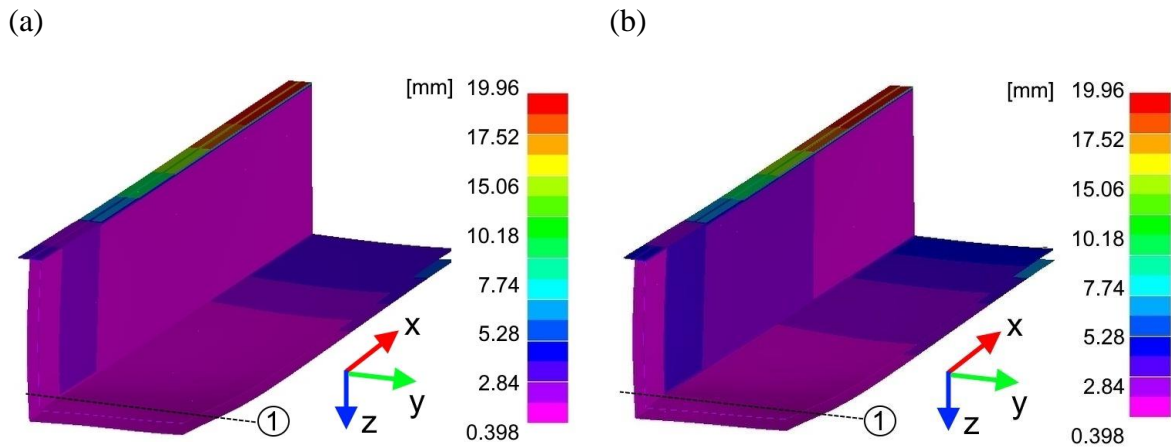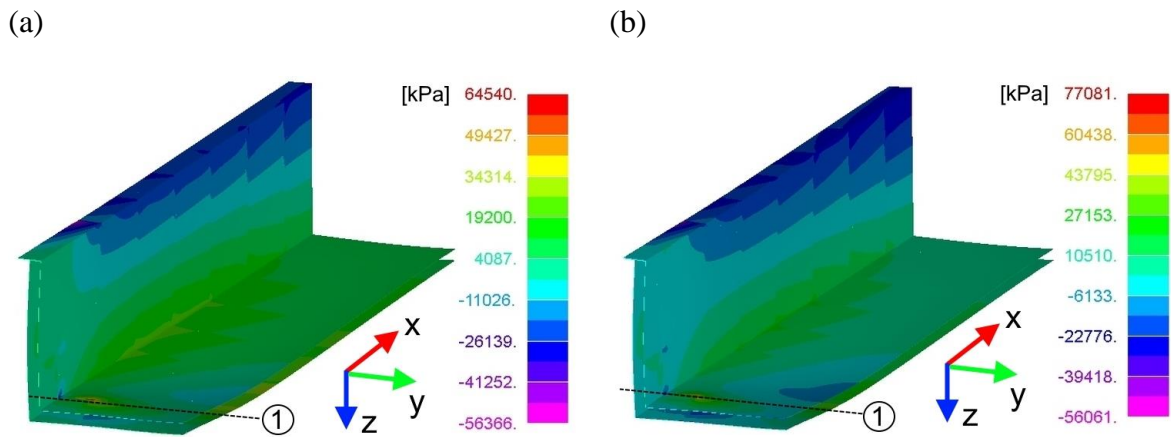Fig. 9. Obtained thicknesses in step I for models: (a) ISO, (b) ORTHO

(a)   (b)

Fig. 10. Obtained longitudinal stresses in step I for models: (a) ISO, (b) ORTHO

4.3. Results for step II

In the second step, constraints for design variable was established in the same way as in the first one, but limits for stresses were introduced as well. That limits were, respectively:

$$\begin{aligned}-25,20\,\text{MPa} &\le \sigma_e \le 13,40\,\text{MPa} \quad \text{for model ISO}\\ -26,02\,\text{MPa} &\le \sigma_e \le 16,64\,\text{MPa} \quad \text{for model ORTHO}\end{aligned},$$

(8)

where σ_e is longitudinal stress in each finite element. The values of limits were taken after the values of stress obtained from models ISO and ORTHO, respectively, before optimization process. Those values also fulfil requirement for FI < 0.2 according to Tsai-Wu hypothesis. After that, for both models, results are presented in Fig. 11 and Fig. 12 respectively.

In model ISO (Fig. 11), the smallest value of thickness obtained in segments S3 and S4 is 2,38 mm, which is about 40% less than initial value. Subsequently, moving to the mid-span the value of thickness increase to finally reach the maximum in segments S7 and S8, where laminate thickness in handrail and platform needs to be greater than initial value. It is presented in Fig. 11b precisely. Horizontal axis represents number of segment (support on the left and mid-span on the right), while vertical axis shows relative change of thickness in each area.

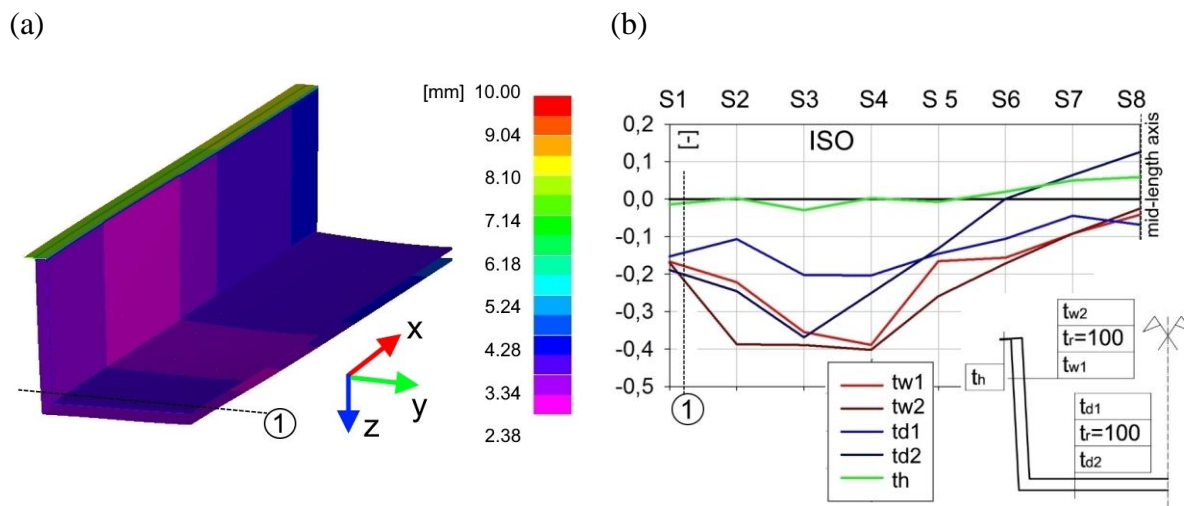(a)   (b)

Fig. 11. Model ISO after step II: (a) obtained thicknesses, (b) relative change of thickness of laminates in each area along footbridge

On the other hand, results for model ORTHO are more complicated (Fig. 12). The smallest value of thickness is 1,012 mm which is about 70% less than initial value. However, in segment S2, which is between 0.5 m and 1.5 m from support, thickness of laminates in walls increase up to

20%. It is because principal stresses are orientated +/-45 degrees comparing to longitudinal direction.

(a)   (b)
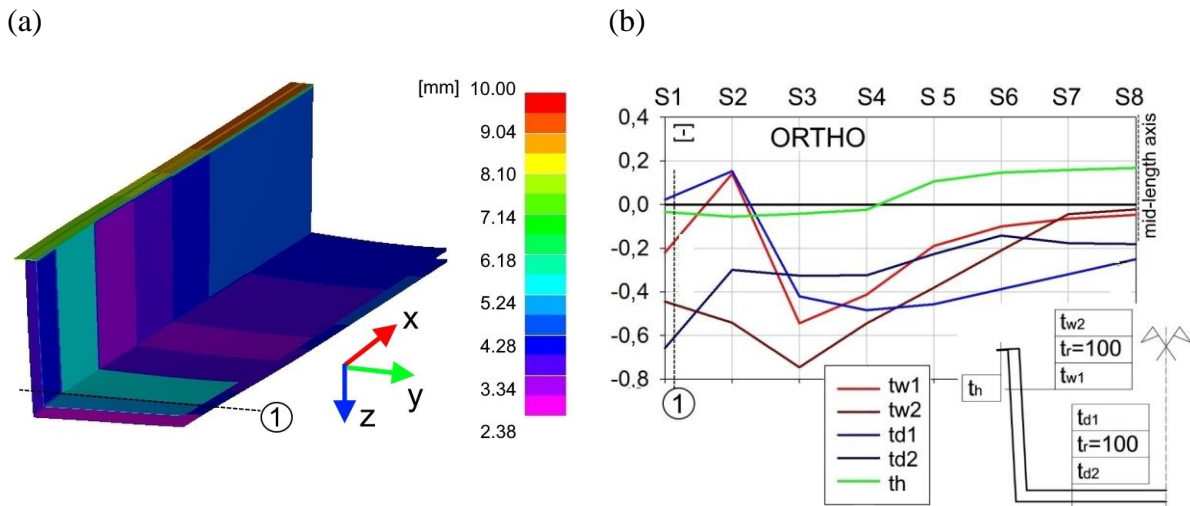

Fig. 12. Model ORTHO after step II: (a) obtained thicknesses, (b) relative change of thickness of laminates in each area along footbridge

Furthermore, Fig. 13 presents longitudinal stress value to check if its level does not go out of the scope.
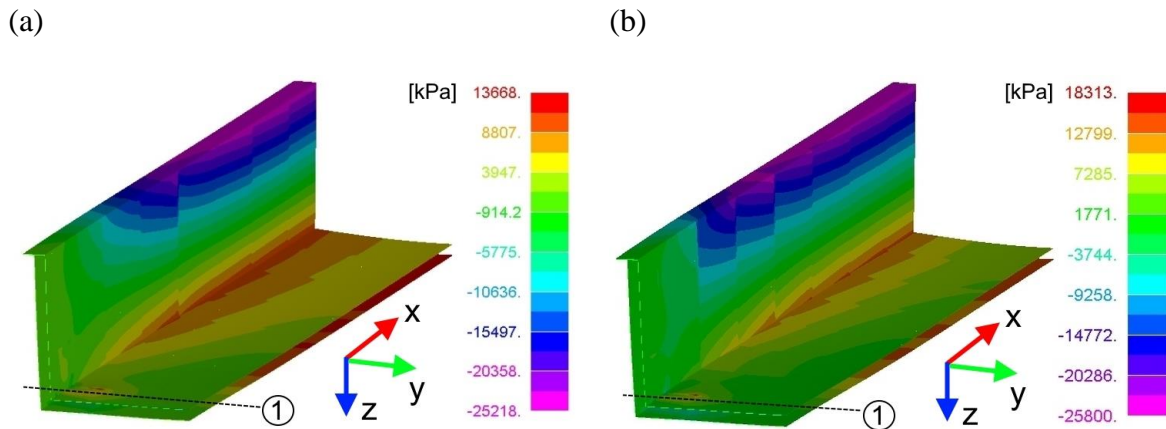
(a)   (b)

Fig. 13. Obtained longitudinal stresses in step II for models: (a) ISO, (b) ORTHO

4.4. Results for step III – the final one

The first and the second step of optimization gave same information how thickness of laminates of designed footbridge can be modified, however in theoretical way. That is why, the third and the last variant was conducted. This is the one in which acceptable range of design variable was established in order to meet technological requirements. Thus i-th design variables, which are the thicknesses of laminates in each area, can exceed values that are result of multiplication of the thickness of single ply, which is 0.663 mm. The smallest number of plies was assumed as 4 due to technological reasons and, successively, that number can increase to 5, 6, 7, 8,… etc. On the other hand, on handrails, the minimum number of plies is 8 and, analogously, can increase. In handrails the number of plies is always at least a sum of the plies in inner and outer laminates in wall as an effect of their overlap ($t_h \geq t_{w1} + t_{w2}$).

Results for both models, ISO and ORTHO, were presented in Fig. 14 and Fig. 15 respectively. The conclusion based on the results obtained in step III are similar to the one from step II, however, the results are slightly different due to new requirement for laminate thickness, which can only take values as a multiplication of single ply.

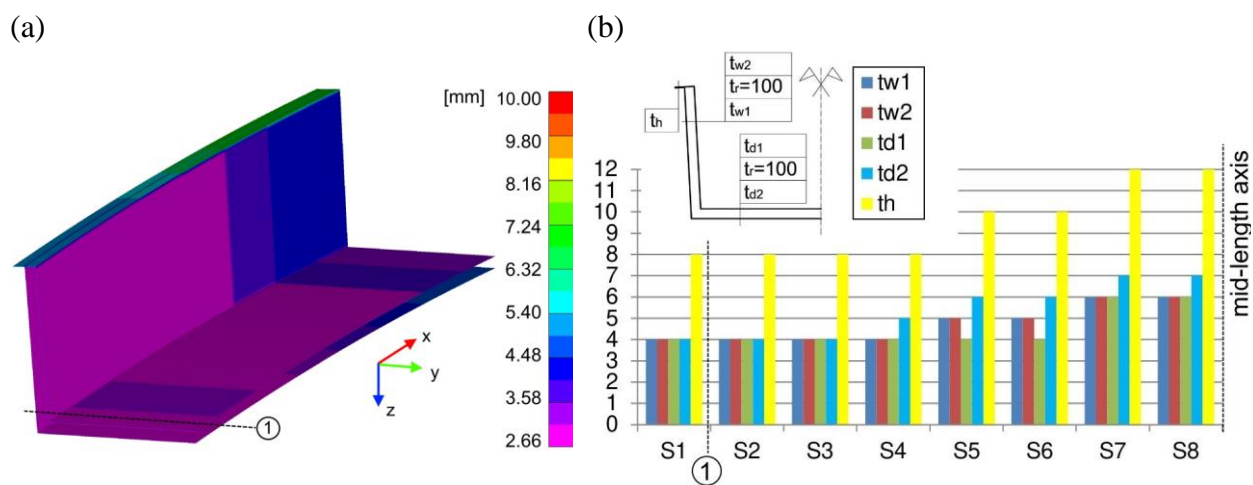(a)   (b)

Fig. 14. Model ISO after step III: (a) obtained thicknesses [mm], (b) number of plies of laminates in each area along footbridge
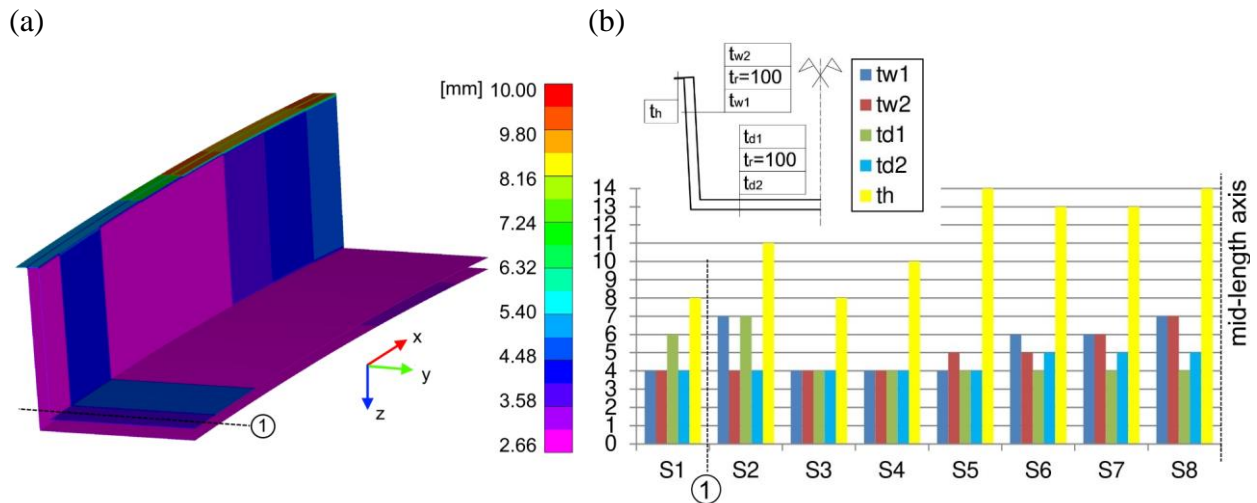
Fig. 15. Model ORTHO after step III: (a) obtained thicknesses [mm], (b) number of plies of laminates in each area along footbridge

In model ISO (Fig. 14), in segments S1-S4 number of plies in almost each area decreased to the minimum value which is 4 in walls and platform deck, and 8 in handrails. Subsequently, considering segments closer to mid-span length the value of required number of plies in walls and platform deck increased and, finally, reached the initial value of 6 and even 7 in outer laminate in deck in segment S8. Analogously the number of plies in handrail increased from the initial value to 12 in segments S7 and S8. Number of plies along structure in each area are shown precisely in Fig. 14b. As before, horizontal axis represents number of segment, while vertical axis shows required number of plies.

The results for model ORTHO (Fig. 15) are more complicated, as it was after step II. Instead of minimum number of plies near support, the number increased up to 7 in inner wall and platform deck in segment S2. As before, that is because principal stresses in those areas are orientated +/-45 degrees comparing to longitudinal direction (x axis). In this situation, the orthogonal material is the weakest hence the number of plies have to be increased. In further analysis of model ORTHO, instead of changing only thickness of laminates, the change of laminate orientation can be pondered as well.

Furthermore, the results show how important is to assume the accurate material model. The results obtained from models ISO and ORTHO are significantly different. It is only theoretical consideration, because, in fact, areas of multilayered laminate of studied footbridge behave more like quasi-isotropic material than orthotropic one. Thus, results for model ISO were chosen as the final one to be implemented in whole structure analysis.

5. Study of footbridge after optimization and comparison to the initial one

Conducted numerical example allowed to determine areas in which thickness of laminate can be decreased and which, at the same time, have to be increased. Optimization process determined the new number of plies. The basic footbridge (model ORTHO6) has 6 plies of laminates along whole structure, 12 plies in handrails, with specified stack sequence. Hence in the footbridge after optimization (model ORTHO6-opt) a distinction of the new stack sequence has to be made. Based on results obtained for model ISO after step III as a required number of plies (Fig. 14), the new stack sequence in each areas were specified and listed in Table 4. As before, BAT is a ply with fibers orientation (0/90) while GBX with (+45/-45).

Table 4. Stack sequence of laminates depending on the number of plies.

Number of plies	Stack sequence
4	[BAT/GBX/GBX/BAT]
5	[BAT/GBX/BAT/GBX/BAT]
6	[BAT/GBX/BAT$_2$/GBX/BAT]
7	[BAT/GBX/BAT$_3$/GBX/BAT]
8	[BAT/GBX/GBX/BAT]$_2$
10	[BAT/GBX/BAT/GBX/BAT]$_2$
12	[BAT/GBX/BAT$_2$/GBX/BAT]$_2$

In order to obtain results for structure that might be not symmetrical, like the one from modal analysis, whole footbridge was analyzed (Fig. 16). Due to analysis of whole structure total number

of nodes and elements increased to 710.423 and 840.828 respectively. Colors represent different type of stack sequence according to Table 4. Additionally, Fig. 17-Fig. 19 contain projections: side view, view from the bottom and view from the top which graphically present stack sequence in each area of structure.
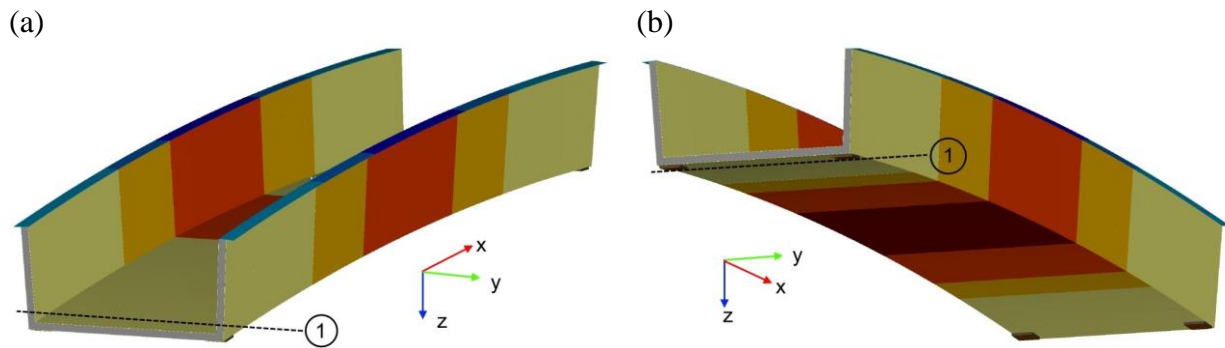
(a) (b)

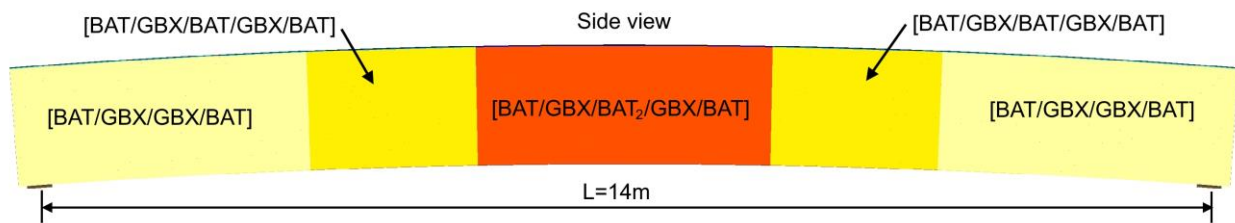Fig. 16. Visualization of whole footbridge (a) view from the right-top, (b) view from the right-bottom

Fig. 17. Side view on footbridge on both sides of walls (tw1 and tw2)
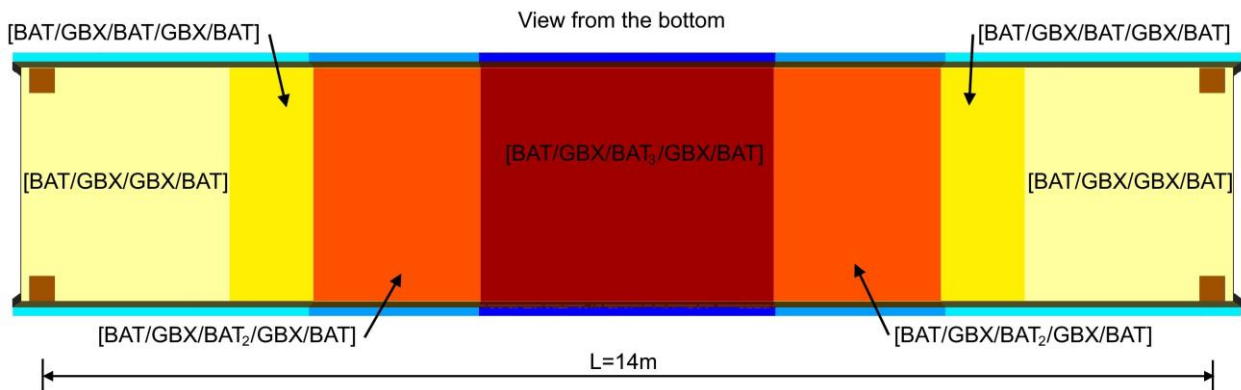

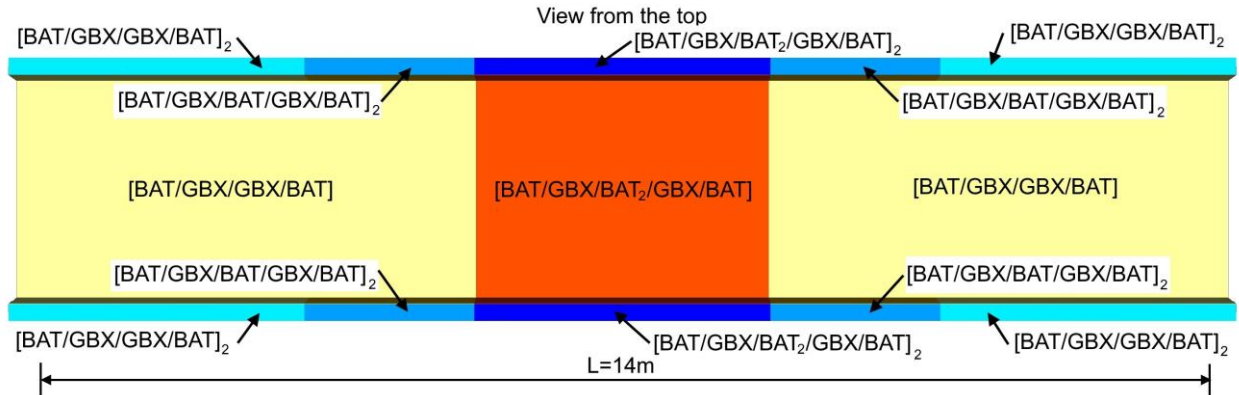Fig. 18. View from the bottom on outer platform deck (td2)

Fig. 19. View from the top on inner platform deck (td1) and handrails (th)

The model after optimization ORTHO6-opt was subject to the same load as previous models, which is $q_t = 5$ kN/m^2 applied on platform deck. Simulated deformation of structure is presented in Fig. 20a. Maximum deflection occur in the middle of span length. The value $v_z = 36.57$ mm compared to theoretical length of the footbridge is about 0.26%, which is equivalent to about $l/380$. Moreover, extreme horizontal displacement of the walls in a transverse direction to interior of structure is $v_y = 32.11$ mm. Additionally, Fig. 20b show the map of longitudinal stress. The obtained values are in the range of $\langle -28,59 ; 11,79 \rangle$ MPa. What has to be mentioned, some discontinuities can be observed due to the variation of laminates thickness as a result of different number of plies along structure. What is obvious, the closer to the middle of the length of a single-span footbridge, the higher the stress level. However, in places where the number of laminate plies increases, the stress level decreases. Hence there is no one global maximum of stress level in the middle of span length, but instead stress in distributed along whole length of structure.

Additionally, obtained values of maximum deformation v_z, strain ε_{x1} and ε_{y2} were compared and listed in Table 5 for model before (ORTHO6) and after optimization (ORTHO6-opt). Due to modular solution in which laminate can adopt only modular thickness, conducted optimization leads to decrease maximum displacement and stains in chosen points.
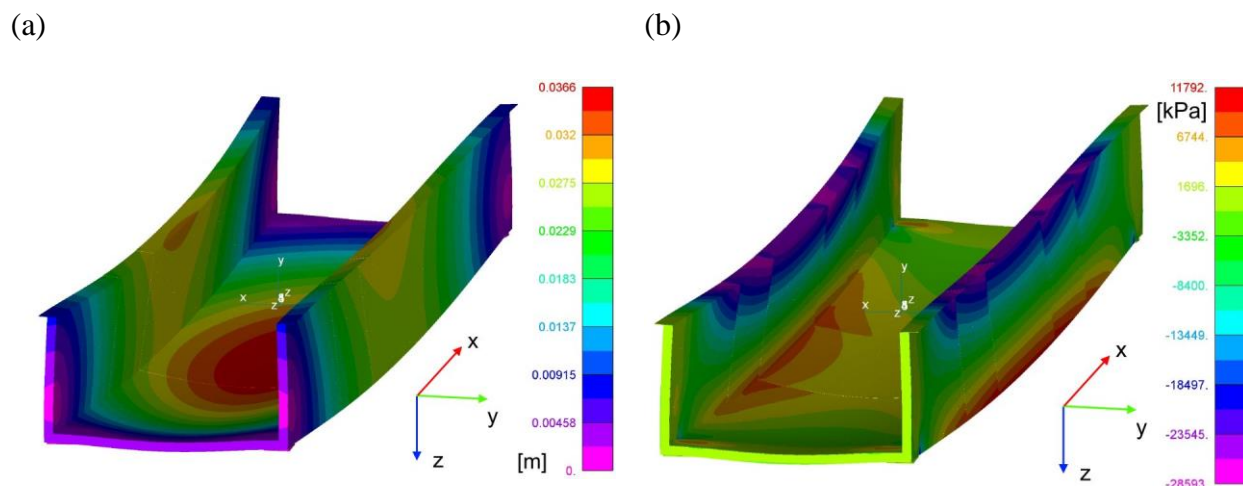
(a) (b)

Fig. 20. Whole footbridge under q_t loading (a) deformation, (b) longitudinal stress

Table 5. Comparison of values obtained from various models

| Model	v_z [mm]	ε_{x1} [µm/m]	ε_{y2} [µm/m]
ORTHO6	38.75	-1215.0	507.9
ORTHO6-opt	36.57	-1085.3	448.0

Although most of the laminates decreased their thickness, the thickness of outer laminate in mid-span length on platform was increased by adding one ply. It can be observed how significant the sensitivity analysis can be. It give the answer how the variation of each design variable can impact of variation of state variable [48].

Additionally, modal analysis was conducted to obtain the values of natural frequencies and corresponding mode shapes of vibrations. Obtained mode shapes are analogous in both models and are presented in Fig. 21. This led to compare corresponding natural frequencies of free vibrations and those values were listed and compared in Table 6.
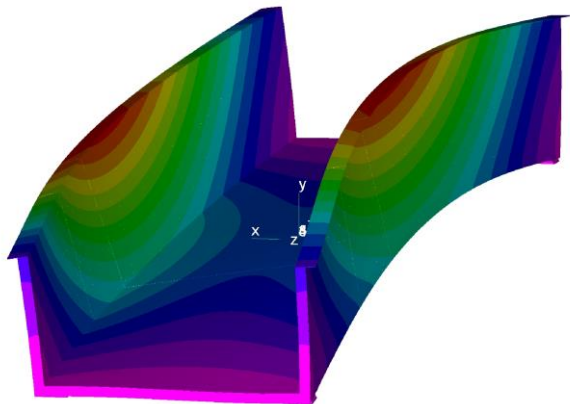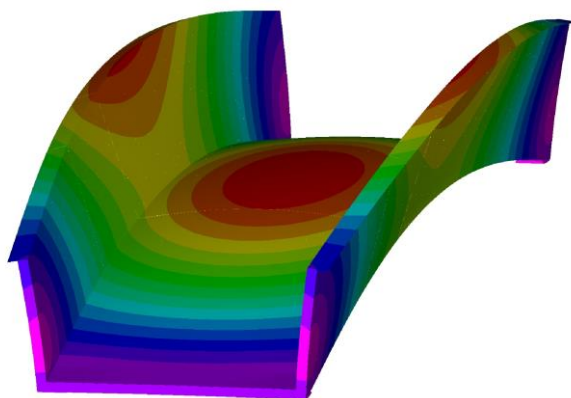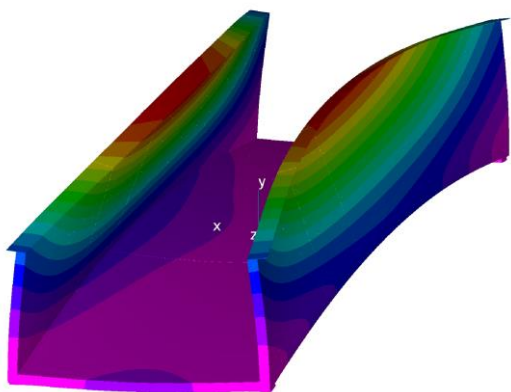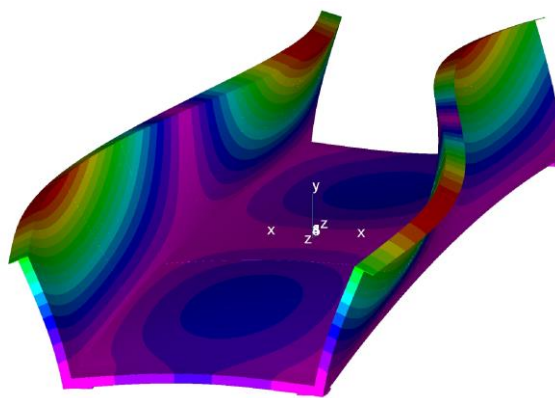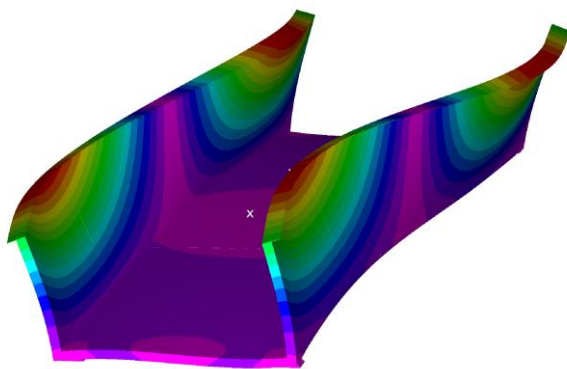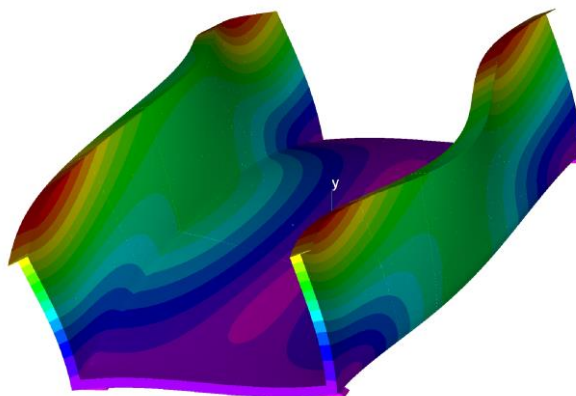
Fig. 21. Six mode shapes obtained in model ORTHO6 and ORTHO6-opt

Table 6. Comparison of frequencies obtained from various models

| Mode shape | Frequency [Hz] | |
	ORTHO6	ORTHO6-opt
1	7.52	7.72
2	10.34	10.38
3	11.80	12.26
4	13.16	14.87
5	13.35	14.96
6	16.04	17.93

As presented, level of frequencies in model after optimization are 2.7% higher in model ORTHO-opt, which is more favorable while designing footbridges in order to avoid resonance caused by walking pedestrians. Although less material were used to manufacture analyzed footbridge, its parameters are improved comparing to the one before optimization. Obtained displacements and strains are lower, at the same time frequencies are higher.

6. Conclusions

The paper focused on parametric optimization of U-shaped composite footbridge.

The reference point for presented solution was footbridge which was design and manufactured and is currently in use (Fig. 3). The parameters for optimization – stress and displacement limits were adopted in the basis of the values obtained in the computational model of realized composite footbridge. This reference allows to assess the benefits of conducted optimization procedures in design process.

The optimal solution was obtained with the reduction of mass of multilayered laminates, faces in sandwich structure, by 18.2%. The optimal solution, received in step 3, meets the conditions of modularity of faces' thickness changes – one ply of laminate is 0.663 mm thick, which is necessary condition for realizations of the structure. Moreover, the minimum thickness of laminates in each

segment was assumed as t_{min}=2.652 mm which is the thickness of four-layered laminate. This is due to technological requirements of infusion process.

The optimal solution, taking onto account the modularity of the thickness of laminates, is characterized by a reduction of the maximum deflection of the structure by 5.6% and an increase of the value of natural frequency of free vibrations by 2.7%. Both values of structural response indicate an increase of the stiffness of the footbridge with reduced mass.

Generally, footbridges are a special structures where often problems with their use occur, mainly considering dynamic response – the structure can be induced into vibrations. Pedestrian traffic generates variable dynamic loads with frequency n_f=2.0÷2.5 Hz. In the case of analyzed footbridge, the first natural frequency of free vibrations is n_1=7.52 Hz and n_{1opt}=7.72 Hz for realized and the optimized footbridge, respectively. There is therefore no fear of resonance.

The cross-section of the structure is U-shaped and has the characteristics of an open thin-walled section. Therefore, the torsional stiffness of the structure has to be verified. That parameter can be assessed by checking the lowest natural frequency of free vibrations corresponding to the torsional mode shape. In this case, torsional mode shape is the fifth mode shape and the corresponding value of frequency is n_{5opt}=14.96 Hz. This value is 193.8% higher than the first natural frequency of free vibrations, hence there is no risk of occurrence of torsional vibrations under environmental load (wind) or utility load (pedestrian and cyclic load).

Finally, the realized footbridge was manufactured on a specially made mold that enables serial production. Hence the benefits obtained from presented optimization can be multiplied and give significant cost reduction.

Optimization and sensitivity analysis, as a part of theory of design, provide the designer a significant support at the design process of structures. Moreover, sensitivity analysis can be effectively used in issues related to strengthening or modernizing structures as well as in the process

of identifying parameters describing the computational model. The obtained solutions always need to be assessed by the designer.

References

[1]   Asby M., Jones D (1999) Engineering Materials 1, Butterwoth-Heinemann, England

[2]   Harris B. (1999) Engineering Composite Materials, The Institute of Materials, London

[3]   Lemaitre J. (2001) Handbook of Materials Behavior Models. Academic Press, France

[4]   Hu N. (2012) Composite and their Properties, http://dx.doi.org/10.5772/2816

[5]   Correia, J. R. (2014). Fibre-Reinforced Polymer (FRP) Composites. Materials for Construction and Civil Engineering, 501–556. doi:10.1007/978-3-319-08236-3_11.

[6]   Potyrała, P. B. & Rius, J. R. C. (2011). Use of fibre reinforced polymer composites in bridge construction. State of the Art in Hybrid and All-Composite Structures. Escola Tecnica Superior d'Enginyers de Camins, Canals i Ports de Barcelona. Universitat Politècnica de Catalunya, Departament Enginyeria de la Construcció.

[7]   Keller, T. (2002). Overview of Fibre-Reinforced Polymers in Bridge Construction. Structural Engineering International, 12(2), 66–70. doi:10.2749/101686602777965595.

[8]   Ascione F., Lamberti M., Razaqpur G. (2015) Modifications of standard GFRP sections shape and proportions for improved stiffness and lateral-torsional stability. Composite Structures 2015, 265-289, 132 doi: 10.1016/j.compstruct.2015.05.005

[9]   Braestrup, M. W. (1999). Footbridge Constructed from Glass-Fibre-Reinforced Profiles,

        Denmark. Structural Engineering International, 9(4), 256–258.

        doi:10.2749/101686699780481709.

[10]   Harvey, W. J. (1993). A Reinforced Plastic Footbridge, Aberfeldy, UK. Structural

        Engineering International, 3(4), 229–232. doi:10.2749/101686693780607589

[11]   Areiza Hurtado, M., Bansal, A., Paulotto, C., &Primi S. (2012). FRP girder bridges:

        Lessons learned in Spain in the last decade, Proceedings of the 6th International Conference

        on FRP Composites in Civil Engineering (CICE-6), Rome, Italy.

[12]   Siwowski, T., Kaleta, D., & Rajchel, M. (2018). Structural behaviour of an all-composite

        road bridge. Composite Structures, 192, 555–567. doi:10.1016/j.compstruct.2018.03.042.

[13]   Piatek, B. & Siwowski, T (2017). Research on the new CFRP prestressing system for

        strengthening of RC structures. Architetecture Civl Engrineering Environment. Vol. 10, 3,

        81-87

[14]   Kulpa M. & Siwowski T. (2018). Stiffness and strength evaluation of a novel FRP

        sandwich panel for bridge redecking. Composite Part B, 167, 207-220. doi:

        10.1016/j.compositesb.2018.12.004

[15]   Brent R., Algorithms for Minimization without Derivatives, Prentice–Hall,1973

[16]   Haug E.J., Arora J.S., Applied Optimal Design, New York-Chichester-Brisbane-Toronto,

        John Wiley and Sons, 1979.

[17]   Nocedal J., Wright S.J., Numerical Optimization, Springer, 1999

[18]   Nikbakt S., Kamarian S., Shakeri M. (2018) A review on optimization of composite

        structures Part I: Laminated composites, Composite Structures 195 (2018) 158–185, doi:

        10.1016/j.compstruct.2018.03.063

[19] Kenichi Ikeya, Masatoshi Shimoda, Jin-Xing Shi (2016) Multi-objective free-form optimization for shape and thickness of shell structures with composite materials, Composite Structures 135 (2016) 262–275, doi: 10.1016/j.compstruct.2010.09.001

[20] Hao Li, Zhen Luo, Mi Xiao, Liang Gao, Jie Gao (2019) A new multiscale topology optimization method for multiphase composite structures of frequency response with level sets, Computer Methods in Applied Mechanics and Engineering, Volume 356, 2019, 116-144, doi: 10.1016/j.cma.2019.07.020

[21] José Humberto S. Almeida Jr., Lars Bittrich, Tsuyoshi Nomura, Axel Spickenheuer (2019) Cross-section optimization of topologically-optimized variable-axial anisotropic composite structures, Composite Structures 225 (2019) 111150, doi: 10.1016/j.compstruct.2019.111150

[22] Muc A. (1995) Transverse shear effects in shape optimization of thinwalled laminated composite structures, Composite Structures, Volume 32, Issues 1–4, 399-408, doi: 10.1016/0263-8223(95)00058-5

[23] Y. Wua, Eric Lib, Z.C. Hea, X.Y. Lina, H.X. Jianga (2020) Robust concurrent topology optimization of structure and its composite material considering uncertainty with imprecise probability, Comput. Methods Appl. Mech. Engrg. 364 (2020) 112927, doi: 10.1016/j.cma.2020.112927

[24] Heng Zhang, Xiaohong Ding∗, Hao Li, Min Xiong (2019) Multi-scale structural topology optimization of free-layer damping structures with damping composite materials, Composite Structures 212 (2019) 609–624, doi: 10.1016/j.compstruct.2019.01.059

[25] Yaoyao Yea, Weidong Zhua, Junxia Jianga, Qiang Xua, Yinglin Kea (2020) Design and optimization of composite sub-stiffened panels, Composite Structures 240 (2020) 112084, doi: 10.1016/j.compstruct.2020.112084

[26] Sabik A., Kreja I. (2011) Stability analysis of multilayered composite shells with cut-outs, ARCHIVES OF CIVIL AND MECHANICAL ENGINEERING, Vol. XI, 2011, No. 1, doi: 10.1016/S1644-9665(12)60183-6

[27] Xiangtao Ma, Kuo Tian∗, Hongqing Li, Yan Zhou, Peng Hao, Bo Wang (2020) Concurrent multi-scale optimization of hybrid composite plates and shells for vibration, Composite Structures 233 (2020) 111635, doi: 10.1016/j.compstruct.2019.111635

[28] Andre Luis Ferreira da Silva, Ruben Andres Salasa, Emilio Carlos Nelli Silva, J.N. Reddy (2020) Topology optimization of fibers orientation in hyperelastic composite material, Composite Structures 231 (2020) 111488, doi: 10.1016/j.compstruct.2019.111488

[29] Michele Iacopo Izzi, Marco Montemurro, Anita Catapano, Jérôme Pailhès (2020) A multi-scale two-level optimisation strategy integrating a global/local modelling approach for composite structures, Composite Structures 237 (2020) 111908, doi: 10.1016/j.compstruct.2020.111908

[30] Yuan Chen, Kunkun Fu, Shujuan Hou, Xu Han, Lin Ye (2018) Multi-objective optimization for designing a composite sandwich structure under normal and 45° impact loadings, Composites Part B 142 (2018) 159–170, doi: 10.1016/j.compositesb.2018.01.020

[31] Yabo Wang , Jianyang Yu, Yanping Song , Fu Chen (2020) Parameter optimization of the composite honeycomb tip in a turbine cascade, Energy 197 (2020) 117236, doi: 10.1016/j.energy.2020.117236

[32] Mazurkiewicz Ł., Małachowski J., Baranowski P. (2015) Optimization of protective panel for critical supporting elements, Composite Structures 134 (2015) 493–505, doi: 10.1016/j.compstruct.2015.08.069

[33] Mazurkiewicz Ł., Małachowski J., Damaziak K., Tomaszewski M. (2018): Evaluation of the response of fibre reinforced composite repair of steel pipeline subjected to puncture

from excavator tooth, Composite Structures 202 (2018) 1126–1135, doi: 10.1016/j.compstruct.2018.05.065

[34] Chróścielewski, J., Miśkiewicz, M., Pyrzowski, Ł. & Wilde, K. (2017). Composite GFRP U-Shaped Footbridge. Polish Maritime Research, 24(s1). doi:10.1515/pomr-2017-0017

[35] Pyrzowski Ł (2018) Testing Contraction and Thermal Expansion Coefficient of Construction and Moulding Polymer Composites, Polish Maritime Research, vol. 25, no. s1, pp. 151–158, doi: 10.2478/pomr-2018-0036

[36] Pyrzowski, Ł., Sobczyk, B., Witkowski, W., & Chróścielewski, J. (2016). Three-point bending test of sandwich beams supporting the GFRP footbridge design process—validation. Advances in Mechanics: Theoretical, Computational and Interdisciplinary Issues, 489–492. doi:10.1201/b20057-104.

[37] Chróścielewski J., Ferenc T., Mikulski T., Miśkiewicz M., Pyrzowski Ł.: Numerical modeling and experimental validation of full-scale segment to support design of novel GFRP footbridge, COMPOSITE STRUCTURES. Vol. 213, (2019), pp.299-307, DOI: 10.1016/j.compstruct.2019.01.089

[38] Miśkiewicz M., Daszkiewicz K., Ferenc T., Witkowski W., Chróścielewski J.: Experimental tests and numerical simulations of full scale composite sandwich segment of a foot- and cycle- bridge, W: 3rd Polish Congress of Mechanics (PCM) / 21st International Conference on Computer Methods in Mechanics (CMM), 2016, Taylor & Francis Group.

[39] Chróścielewski J., Miśkiewicz M., Pyrzowski Ł., Sobczyk B. & Wilde K. (2017) A novel sandwich footbridge - Practical application of laminated composites in bridge design and in situ measurements of static response, Composites Part B 126, 153-161

[40] Chróścielewski J., Miśkiewicz M., Pyrzowski Ł., Rucka M., Sobczyk B. & Wilde K (2018) Modal properties identification of a novel sandwich footbridge – Comparison of measured dynamic response and FEA, Composites Part B 151, 245-255

[41] Tsai S. W. & Wu E. M. (1971) A general theory of strength for anisotropic materials, J. Comp. Mater. 5 (1)

[42] Tsai S. W &, Hahn H. T. (1980) Introduction to composite materials, Technomic Publishing Co., Lancaster, USA

[43] Chróścielewski J, Klasztorny M, Nycz D, Sobczyk B. (2014) Load capacity and serviceability conditions or footbridges made of fibre-reinforced polymer laminates. Roads Bridges;13,189-202. http://dx.doi.org/10.7409/rabdim.014.013

[44] Małachowski J, L'vov G, Daryazadeh S. (2017) Numerical prediction of the parameters of a yield criterion for fibrous composites. Mechanics of Composite Materials, 53, 589–600. http://dx.doi.org/10.1007/s11029-017-9689-1.

[45] Chróścielewski J, Klasztorny M, Romanowski R, Barnat W, Małachowski J, Derewońko A, et al. (2015) Badania eksperymentalne identyfikacyjne kompozytu. Raport z realizacji podzadania 5.1 WAT (internal report), Warsaw (in Polish)

[46] Reddy, J. N. (1984) A simple higher-order theory for laminated composite plates, Journal of Applied Mechanics, Trans. ASME, Vol. 51, 745-752

[47] Sabik A. & Kreja I. (2008) Linear analysis of laminated multilayered plates with the application of zig-zag function. Archives of Civil and Mechanical Engineering, 8, 61-72

[48] Ferenc T., Pyrzowski Ł., Chróścielewski J. & Mikulski T. (2018) Sensitivity analysis in designing process of sandwich U-shaped composite footbridge, Shell Structures: Theory and Applications. - Vol. 4, ed. W. Pietraszkiewicz, W. Witkowski, Leiden: CRC Press/Balkema, 413-416